Appendix 1 Supplemental methods

Single-cell RNA sequencing analysis

We obtained two single-cell RNA sequencing databases for E-MTAB-6149 (45) through https://www.ebi.ac.uk/ and PRJNA482529 (46) via https://www.ncbi.nlm.nih.gov/. The raw matrices of gene expression per sample were created using CellRanger and then transformed into a Seurat object utilizing the Seurat R package (47). Subsequently, we excluded all cells with fewer than 500 expressed characteristics, over 20% expression of mitochondrial genes, over 1% expression of hemoglobin genes, and less than 1000 total RNA counts. This was done with the aim of ensuring the quality of data for subsequent analysis. The integration of data from single cells across multiple samples was executed using the Harmony package (48). Identification and elimination of doublets were performed using the DoubletFinder R package (49).

To diminish the dataset's dimensionality, we employed principal component analysis to summarize the variably expressed genes. The first 20 principal components were further condensed using tSNE dimensionality reduction, utilizing the default settings of the RunTSNE function within the Seurat package. Employing the graph-based clustering approach in the Seurat package's FindClusters function, with a conservative resolution of 0.5 and default parameters otherwise, each cell type was reclustered based on its principal components. Subsequently, cell clusters in the resulting two-dimensional representation were assigned annotations corresponding to known biological cell types using canonical marker genes.

In the context of epithelial cells, we specifically implemented dimensionality reduction via principal component analysis on variably expressed genes, as previously described. The graph-based clustering approach within the Seurat package's FindClusters function was then applied, with a conservative resolution of 0.2 and default parameters otherwise, to recluster each cell type based on its principal components. To aid visualization, these informative principal components were transformed into tSNE plots as outlined above.

For the analysis of single-cell data, we conducted differential gene analysis using the FindMarkers function within the Seurat package. Furthermore, we explored copy number variations in single-cell data using the infercnv R package.

Laboratory experimental overview

Cell lines and cell culture

The A549 and HEK293T cell lines were sourced from the American Type Culture Collection (ATCC; USA). Maintaining adherence to recommended practices, all cells were cultured at 37 ℃ in a 5% CO_2 environment using the appropriate medium (DMEM) supplemented with 10% fetal bovine serum (FBS) and 1% penicillin and streptomycin (p/s).

Stable transfections

Lentiviral vectors encoding short hairpin RNA targeting human NET1 (shNET1) and a scramble control shRNA were developed by Gene Pharma Corporation, located in Shanghai, China. The sequence for shNET1 is as follows: Forward (5'-3') - CCGGCGCCTAGTCAAATACCCTTTACTCGAGTAAAGGGTATTTGACTAGGCGTTTTTG, Reverse (5'-3') – AATTCAAAAACGCCTAGTCAAATACCCTTTACTCGAGTAAAGGGTATTTGACTAGGCG.

Immunohistochemistry (IHC) staining

NSCLC tumor samples and corresponding resection margin tissues were fixed, dehydrated, and embedded in paraffin before being sectioned to a thickness of 4 μm. The sections were then incubated with NET1 primary antibodies (Sigma-Aldrich HPA020068) at a 1:150 dilution. NET1 expression was quantified by analyzing three randomly selected fields at 40x magnification per sample. The proportion of NET1-positive cells was determined through microscopic evaluation and classified into the following categories: score 0 for 0–5% positive cells, score 1 for 5–24% positive cells, score 2 for 25–49%, score 3 for 50–74%, and score 4 for 75% or more.

The quantitative real-time PCR (qRT-PCR)

RNA was extracted using TRIzol Reagent (Invitrogen) from cells and the RNeasy FFPE Kit (Qiagen) from FFPE tumor samples and corresponding resection margin tissues.. Subsequently, reverse transcription was carried out using an MLV-

 https://dx.doi.org/10.21037/tcr-24-587

reverse transcriptase kit (Invitrogen). Following this, qRT-PCR was conducted in triplicate assays with SYBR Green (Tiangen, China) on an ABI 7500 Real-Time Detection system (Applied Biosystems), following the manufacturer's protocol. GAPDH was utilized as the internal standard. The experiments were replicated three times, and data analysis was carried out using the $2^{-\Delta\Delta Ct}$ method.

The primer sequences for NET1 were as follows: Forward (5'-3') - CTGTTCACCTCGGGACATTT, Reverse (5'-3') - TGGAGCTGTCAGACGTTTTG. For GAPDH, the primer sequences were as follows: Forward (5'-3') - GAAGGTGAAGGTCGGAGTC, Reverse (5'-3') - GAAGATGGTGATGGGATTTC.

Cell viability

HEK293T and A549 cells were seeded at a density of 3×10^3 cells/well into 96-well culture plates. Following a 1-day, 3-day, and 5-day incubation, 3-(4, 5-dimethylthiazol-2-yl)-2, 5-diphenyltetrazolium bromide (MTT) was introduced into the medium. Incubation at 37 ℃ was carried out for 4 hours. The resulting formazan crystals were dissolved in 150 µL of dimethyl sulfoxide (DMSO), and the optical density was measured to evaluate cell viability using a Microplate Reader (Bio-Rad iMark™, United States) with a test wavelength of 450nm. All cell viability assays were conducted with three biological replicates.

Ferroptosis evaluation via malondialdehyde (MDA) quantification

To assess ferroptosis, MDA levels were measured in different groups using Sigma-Aldrich's Lipid Peroxidation (MDA) Assay Kit (Cat #: MAK085), following manufacturer protocols. This approach enabled the direct comparison of ferroptosis across the groups based on MDA, a lipid peroxidation marker. All MDA assays were conducted with three biological replicates.

Inhibition of ferroptosis in A549 cells using liproxstatin-1 and ferrostatin-1

liproxstatin-1 (Lip-1, #S7699) and ferrostatin-1 (Fer-1, #S7243) were obtained from Selleck Chemicals (Houston, TX, USA).

To inhibit ferroptosis, the A549 cells were treated with Fer-1 (1 µmol/L) or Lip-1 (0.2 µmol/L) for 96 h after the removal of lentiviral vectors (50).

References

45. Lambrechts D, Wauters E, Boeckx B, et al. Phenotype molding of stromal cells in the lung tumor microenvironment. Nat Med 2018;24:1277-89.
46. Song Q, Hawkins GA, Wudel L, et al. Dissecting intratumoral myeloid cell plasticity by single cell RNA-seq. Cancer Med 2019;8:3072-85.
47. Hao Y, Stuart T, Kowalski MH, et al. Dictionary learning for integrative, multimodal and scalable single-cell analysis. Nat Biotechnol 2024;42:293-304.
48. Korsunsky I, Millard N, Fan J, et al. Fast, sensitive and accurate integration of single-cell data with Harmony. Nat Methods 2019;16:1289-96.
49. McGinnis CS, Murrow LM, Gartner ZJ. DoubletFinder: Doublet Detection in Single-Cell RNA Sequencing Data Using Artificial Nearest Neighbors. Cell Syst 2019;8:329-337.e4.
50. Tang Z, Jiang W, Mao M, et al. Deubiquitinase USP35 modulates ferroptosis in lung cancer via targeting ferroportin. Clin Transl Med 2021;11:e390.

https://dx.doi.org/10.21037/tcr-24-587

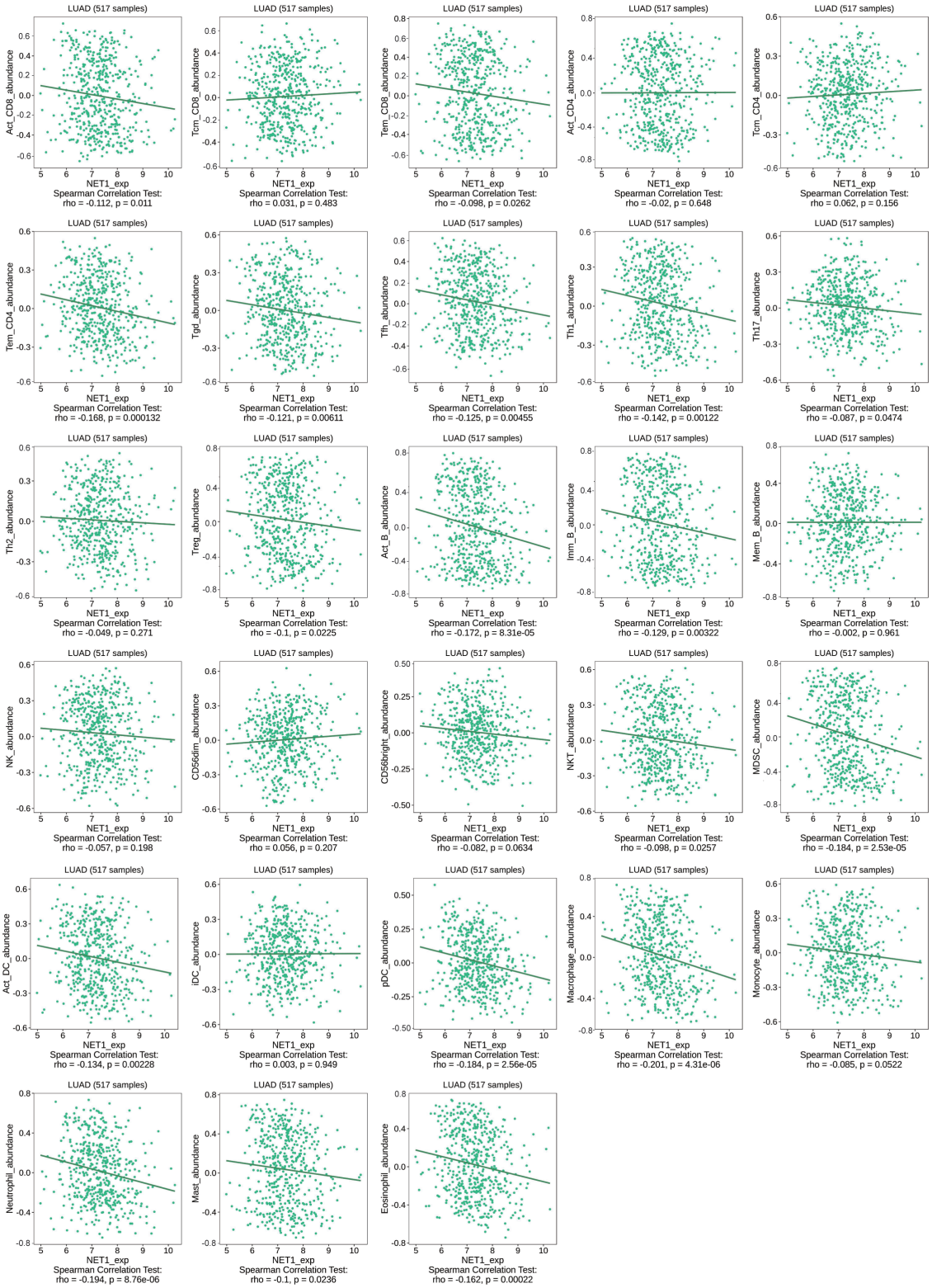

Figure S1 Impact of NET1 on TILs abundance in TCGA-LUAD. The dot plots illustrate the associations between GSVA-derived abundances of 28 types of TILs and NET1 expression across 517 patients with LUAD. NET1: neuroepithelial cell transforming 1; TILs: tumor-infiltrating lymphocytes; TCGA-LUAD: The Cancer Genome Atlas-Lung Adenocarcinoma; GSVA: gene set variation analysis.

https://dx.doi.org/10.21037/tcr-24-587

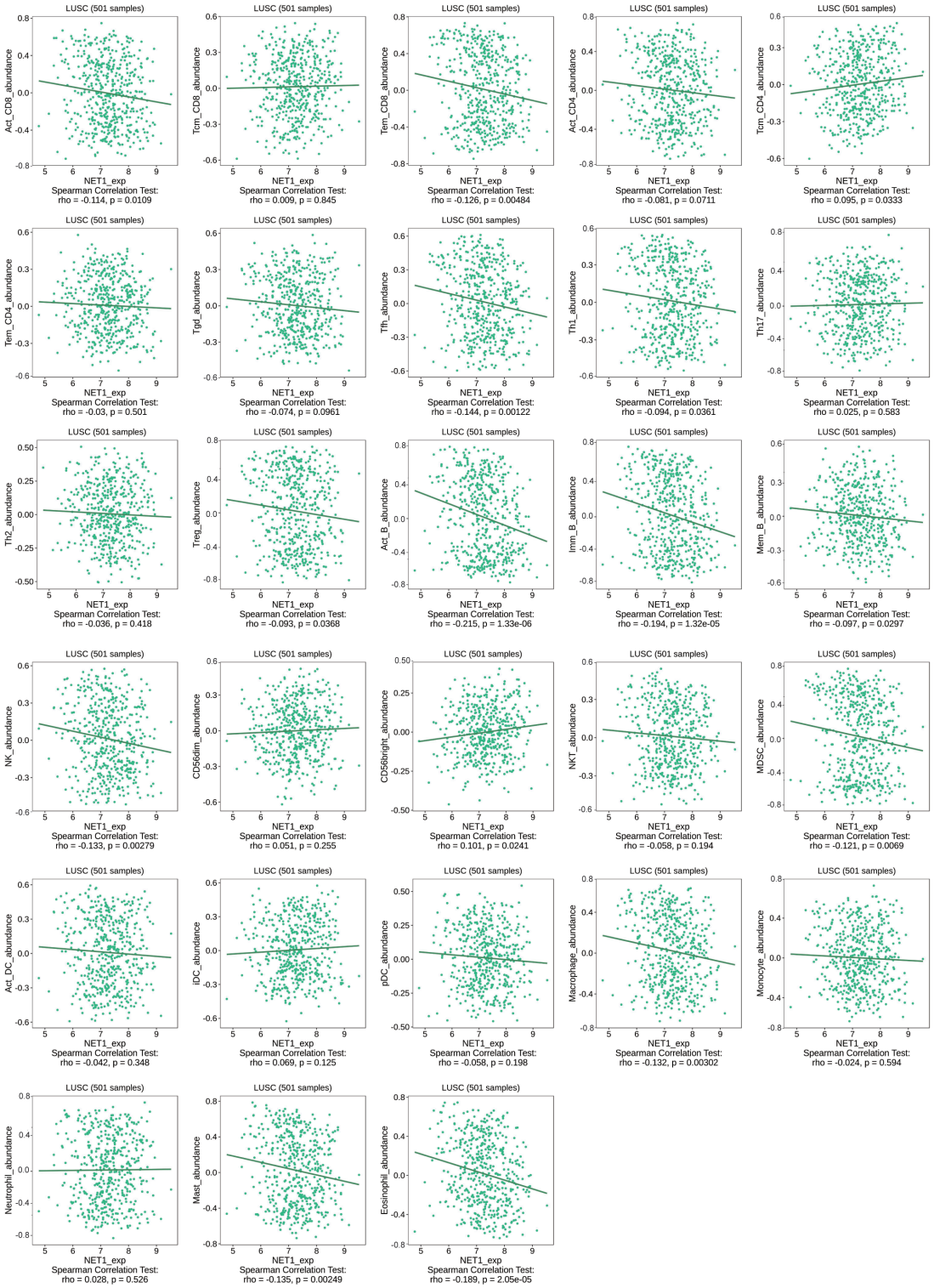

Figure S2 Impact of NET1 on TILs abundance in TCGA-LUSC. The dot plots illustrate the associations between GSVA-derived abundances of 28 types of TILs and NET1 expression across 501 patients with LUSC. NET1: neuroepithelial cell transforming 1; TILs: tumor-infiltrating lymphocytes; TCGA-LUSC: The Cancer Genome Atlas-Lung Squamous Cell Carcinoma; GSVA: gene set variation analysis.

https://dx.doi.org/10.21037/tcr-24-587

Table S1 Clinical characteristics of high and low NET1 expression groups in TCGA-LUAD

Characteristics	High	Low	P
n	258	257	
Diagnosis, age, mean (SD)	65.59 (9.86)	65.02 (10.19)	0.525
Sex, male (%)	119 (46.1)	120 (46.7)	0.967
Smoking (%)			0.259
Current reformed smoker for >15 years	68 (27.1)	67 (26.8)	
Current reformed smoker for ≤15 years	92 (36.7)	75 (30.0)	
Current reformed smoker, duration not specified	3 (1.2)	1 (0.4)	
Current smoker	57 (22.7)	63 (25.2)	
Lifelong non-smoker	31 (12.4)	44 (17.6)	
T-stage (%)			0.187
T1	80 (31.0)	89 (34.6)	
T2	141 (54.7)	136 (52.9)	
T3	24 (9.3)	23 (8.9)	
T4	13 (5.0)	6 (2.3)	
TX	0 (0.0)	3 (1.2)	
N-stage (%)			0.081
N0	177 (68.9)	155 (60.3)	
N1	40 (15.6)	55 (21.4)	
N2	35 (13.6)	39 (15.2)	
N3	2 (0.8)	0 (0.0)	
NX	3 (1.2)	8 (3.1)	
M-stage (%)			0.058
M0	173 (67.6)	172 (67.5)	
M1	7 (2.7)	18 (7.1)	
MX	76 (29.7)	65 (25.5)	
AJCC-Stage (%)			0.067
Stage I	147 (57.9)	129 (51.0)	
Stage II	57 (22.4)	64 (25.3)	
Stage III	43 (16.9)	41 (16.2)	
Stage IV	7 (2.8)	19 (7.5)	

SD, standard deviation; AJCC, American Joint Committee on Cancer; NET1, neuroepithelial cell transforming 1; TCGA-LUAD, The Cancer Genome Atlas-Lung Adenocarcinoma.

https://dx.doi.org/10.21037/tcr-24-587

Table S2 Clinical characteristics of high and low NET1 expression groups in TCGA-LUSC

Characteristics	High	Low	P
n	251	250	
Diagnosis, age, mean (SD)	67.54 (8.77)	66.86 (8.38)	0.375
Sex, male (%)	190 (75.7)	181 (72.4)	0.459
Smoking (%)			0.016
Current reformed smoker for >15 years	54 (21.9)	29 (12.0)	
Current reformed smoker for ≤15 years	118 (47.8)	132 (54.5)	
Current reformed smoker, duration not specified	4 (1.6)	1 (0.4)	
Current smoker	60 (24.3)	73 (30.2)	
Lifelong non-smoker	11 (4.5)	7 (2.9)	
T-stage (%)			0.653
T1	58 (23.1)	56 (22.4)	
T2	141 (56.2)	152 (60.8)	
T3	40 (15.9)	31 (12.4)	
T4	12 (4.8)	11 (4.4)	
N-stage (%)			0.34
N0	168 (66.9)	151 (60.4)	
N1	58 (23.1)	73 (29.2)	
N2	21 (8.4)	19 (7.6)	
N3	1 (0.4)	4 (1.6)	
NX	3 (1.2)	3 (1.2)	
M-stage (%)			0.496
M0	207 (82.8)	204 (82.6)	
M1	5 (2.0)	2 (0.8)	
MX	38 (15.2)	41 (16.6)	
AJCC-Stage (%)			0.651
Stage I	120 (48.4)	124 (49.8)	
Stage II	83 (33.5)	79 (31.7)	
Stage III	40 (16.1)	44 (17.7)	
Stage IV	5 (2.0)	2 (0.8)	

SD, standard deviation; AJCC, American Joint Committee on Cancer; NET1, neuroepithelial cell transforming 1; TCGA-LUSC, The Cancer Genome Atlas-Lung Squamous Cell Carcinoma.

https://dx.doi.org/10.21037/tcr-24-587